Nonlinear Signal Analysis: Time-Frequency Perspectives

T. Kijewski-Correa[1] and A. Kareem[2]

Abstract: Recently, there has been growing utilization of time-frequency transformations for the analysis and interpretation of nonlinear and nonstationary signals in a broad spectrum of science and engineering applications. The continuous wavelet transform and empirical mode decomposition in tandem with Hilbert transform have been commonly utilized in such applications, with varying success. This study evaluates the performance of the two approaches in the analysis of a variety of classical nonlinear signals, underscoring a fundamental difference between the two approaches: the instantaneous frequency derived from the Hilbert transform characterizes subcyclic and supercyclic nonlinearities simultaneously, while wavelet-based instantaneous frequency captures supercyclic nonlinearities with a complementary measure of instantaneous bandwidth characterizing subcyclic nonlinearities. This study demonstrates that not only is the spectral content of the wavelet instantaneous bandwidth measure consistent with that of the Hilbert instantaneous frequency, but in the case of the Rössler system, produces identical oscillatory signature.

DOI: 10.1061/(ASCE)0733-9399(2007)133:2(238)

CE Database subject headings: Nonlinear analysis; Frequency analysis; Time series analysis; Transformation; Oscillations.

Introduction

Time-frequency analyses have received growing acceptance in a variety of engineering and science disciplines, where the limitations of the infinite bases of the Fourier transform have made the investigation of localized or time-varying features impossible. Among the various time–frequency transformations available, the continuous wavelet transform (CWT) (e.g., Kijewski and Kareem 2003) and empirical mode decomposition with Hilbert transform (EMD+HT) (Huang et al. 1998) are among the most popular. As the performance of the former technique was called into question by Huang et al. (1998), and this misinterpretation of results has continued in subsequent publications (e.g., Hwang et al. 2003; Peng et al. 2005), it is important to affirm its appropriateness for the analysis of nonstationary and nonlinear signals. Such an evaluation is reported in part in Kijewski-Correa and Kareem (2006) and is continued here for the case of a number of classical nonlinear systems.

The discussion of performance will focus on two quantities: the analytic signal and the instantaneous frequency $IF(t)$, taken as the derivative of the analytic signal's phase. Space does not permit a detailed discussion of the relevant theory, though one is provided in Kijewski-Correa and Kareem (2006) and textbooks such as Carmona et al. (1998). The analytic signal has been traditionally generated using the Hilbert transform, though, in the case of multicomponent signals, the application of the Hilbert transform must be preceded by a filtering operation to transform the signal to a series of monocomponent signals. Recently it was proposed by Huang et al. (1998) to replace this filtering process by EMD, where a series of monocomponent signals or intrinsic mode functions (IMFs) are generated by a progressive sifting operation detailed in that reference. Alternatively, continuous wavelet transforms of the analytic type can be applied to generate analytic signals representative of the various components within the signal. These analytic signal estimates are drawn from the complex-valued wavelet coefficients along the *stationary points* of the time–frequency map. The stationary points are time-scale ordinates at which the frequency of the scaled wavelet coincides with the local frequency of the signal forming a *ridge* in the time–frequency plane at specific scales, which are inversely proportional to the instantaneous frequency. The details surrounding this theory are provided in a number of texts, including Carmona et al. (1998), which also discusses a number of techniques suitable for the extraction of ridges. Once these ridges are identified: the instantaneous frequency can be extracted by one of two techniques—again directly from the scale values forming the ridges or by taking the derivative of the phase of the analytic signal drawn from the wavelet coefficients along the ridge. One class of analytic wavelet is the Morlet wavelet used in this study, whose bases are comprised of a localized sine and cosine oscillating at a central frequency f_0.

While the notion of frequency at an instant may seem paradoxical, it may be conceptualized as the frequency of a sine wave that locally fits the signal under consideration. As such, it has generally been accepted in the literature as the average frequencies at each point in time (Priestly 1988); the discussion has not fully extended to consider the instantaneous bandwidth or spread of frequencies contributing to this mean. As later examples will

[1]Rooney Family Assistant Professor, Dept. of Civil Engineering and Geological Sciences, Univ. of Notre Dame, 156 Fitzpatrick Hall, Notre Dame, IN 46556 (corresponding author).

[2]Robert M. Moran Professor, Dept. of Civil Engineering and Geological Sciences, Univ. of Notre Dame, 156 Fitzpatrick Hall, Notre Dame, IN 46556.

Note. Associate Editor: Raimondo Betti. Discussion open until July 1, 2007. Separate discussions must be submitted for individual papers. To extend the closing date by one month, a written request must be filed with the ASCE Managing Editor. The manuscript for this technical note was submitted for review and possible publication on September 1, 2005; approved on July 6, 2006. This technical note is part of the ***Journal of Engineering Mechanics***, Vol. 133, No. 2, February 1, 2007. ©ASCE, ISSN 0733-9399/2007/2-238–245/$25.00.

demonstrate, the spread about the instantaneous frequency is as important in shedding light on the nature of the signal being analyzed as the instantaneous frequency itself. In the case of wavelet transforms, at any time t_i, a plot of the squared magnitude of the wavelet coefficients yields an instantaneous spectrum, identifying the dominant components within the system. Each component peaks at its instantaneous frequency value with measurable spread, characterized by the instantaneous bandwidth. Based on the work of Cohen and Lee (1990), let the instantaneous bandwidth of a wavelet instantaneous spectrum $S(f, t=t_i)$ be defined as

$$B^2 = \int_{f_1}^{f_2} [f - IF(t_i)]^2 |S(f, t = t_i)|^2 df \tag{1}$$

where the limits of integration are defined by the frequency range associated with a given spectral peak. The definition of these limits of integration is not generally straightforward for multicomponent signals. As a result, it is suggested herein to make use of the half-power bandwidth (HPBW) estimator β (Bendat and Piersol 1986), since it is concerned only with the spectral peak value. It should be noted that, while the wavelet bandwidth is modified by the window contributions of the parent wavelet (Kijewski-Correa 2003), the HPBW measure can still be used to track the relative variations of instantaneous bandwidth over time.

Applications

The following examples discuss the manner in which CWT and EMD+HT characterize a number of classic nonlinear systems. To aid in this discussion, the concept of *subcyclic* oscillations, denoting changes in frequency that occur within a single cycle of oscillation, is introduced. This is in contrast to *supercyclic* oscillations, denoting changes in frequency that occur over the course of one or more cycles or due to rapid changes in amplitude. For systems possessing supercyclic characteristics, the wavelet will capture these in its instantaneous frequency measure; however, any subtle characteristics of subcyclic frequency variation are not held in this measure. As Priestley (1988) indicated, the instantaneous frequency is an averaged measure of the frequencies present at that instant in time. In the case of the Morlet wavelet, this is essentially the frequency of the best-fit sinusoid to the data over a shortened time window. However, if the signal deviates from the sinusoidal form, sinusoids at neighboring scales also bear some similitude with the signal over this same interval. These deviations, which are often caused by subcyclic frequency modulations, must locally be treated by a summation of neighboring harmonics, whose spread is captured by the instantaneous bandwidth measure defined in Eq. (1) or by the HPBW. On the other hand, the application of the Hilbert transform to a strictly monocomponent signal yields an instantaneous frequency estimate that captures both super and subcyclic oscillations simultaneously. However, it should be noted that the Hilbert transform will inherit any limitations innate to the sifting process, e.g., the residual traces of other frequency components in a given IMF—a potential artifact of the nonorthogonality of the decomposition.

Readers should keep in mind that a proper understanding of each approach and its implementation issues is critical to achieving valid results. For example, the resolution characteristics of the Morlet wavelet are dictated by the central frequency parameter f_0 and greatly impacts this wavelet's ability to detect nonlinear characteristics, as demonstrated in Kijewski-Correa and Kareem (2006) for the case of Stokian waves. The significance of resolution is also highlighted in this study in the case of the Duffing oscillator. Another important consideration is the presentation of results: EMD+HT results are plotted in the form of a Hilbert spectrum, which displays the amplitude of the Hilbert-transformed IMFs as a function of time and instantaneous frequency, estimated from the analytic signal phase. Commonly in the literature, e.g., in Huang et al. (1998), these results are erroneously compared to wavelet scalograms, however, as discussed in Kijewski-Correa and Kareem (2006), the use of wavelet instantaneous frequency spectra (WIFS) insures an equivalent basis for comparison.

Duffing Equation

One of the most well known nonlinear examples is the Duffing oscillator under harmonic excitation described by a second-order differential equation

$$\frac{d^2x}{dt^2} + (1 + \varepsilon x^2)x = \gamma \cos \omega_d t \tag{2}$$

where ε, γ=constants, and ω_d=harmonic forcing frequency. The term in parenthesis represents nonlinearity in the stiffness of the oscillator, which will lead to a frequency that changes with amplitude and displays marked intrawave oscillations of both long and short period (Huang et al. 1998).

The response of the system in Eq. (2) is numerically simulated using a fourth order Runga–Kutta scheme to determine if the wavelet is sensitive enough to detect subtle nonlinearities, embodied by a Duffing oscillator with $\varepsilon=-0.22$, $\gamma=0.1$. For a more basic understanding of the behavior, the system is first released from the initial conditions of $x(0)=0$ and $\dot{x}(0)=1$ and allowed to freely vibrate, as shown in Fig. 1(a). As evidenced by the power spectral density (PSD) to the right of Fig. 1(a), the dominant Fourier frequency is at 0.143 Hz, with an additional peak around 0.425 Hz, which is at three times the primary frequency as a result of the cubic nonlinearity in Duffing equation. The application of a Morlet wavelet with $f_0=0.25$ Hz, in order to achieve a refined temporal resolution, yields a scalogram [Fig. 1(b)] and WIFS [Fig. 1(c)] indicating a concentration of energy near 0.12 Hz. The frequency resolution of the scalogram can be improved by selecting a larger central frequency, e.g., $f_0=2$ Hz (Kijewski and Kareem 2003). The resulting scalogram and WIFS are shown in Figs. 1(d and e), respectively, which concentrate at 0.143 Hz, consistent with the spectral description in Fig. 1(a). The phase of the wavelet transform approximation to the analytic signal can be used to provide a more precise identification of instantaneous frequency, when lower frequency resolution wavelets are applied. This result is shown in Fig. 1(f) for $f_0=0.25$ Hz, identifying a frequency component at 0.143 Hz with oscillatory characteristics described by the accompanying power spectral density, which verifies a dominant frequency of oscillation at 0.145 Hz with a trace of oscillation at approximately twice that frequency. By examining the instantaneous bandwidth for $f_0=0.25$ Hz [Fig. 1(g)], there is additional evidence of the subtle nonlinearity of this system, with its accompanying power spectral representation verifying that this oscillatory characteristic features scales at the instantaneous frequency and twice its value. The fluctuations of bandwidth describe the variation of the spread of frequencies about the instantaneous frequency shown in Fig. 1(f). As the frames in Fig. 1 help to demonstrate, the bandwidth, sensitive to signal amplitude, takes on its lowest values in the signal's troughs and peaks at the zero crossings of the signal,

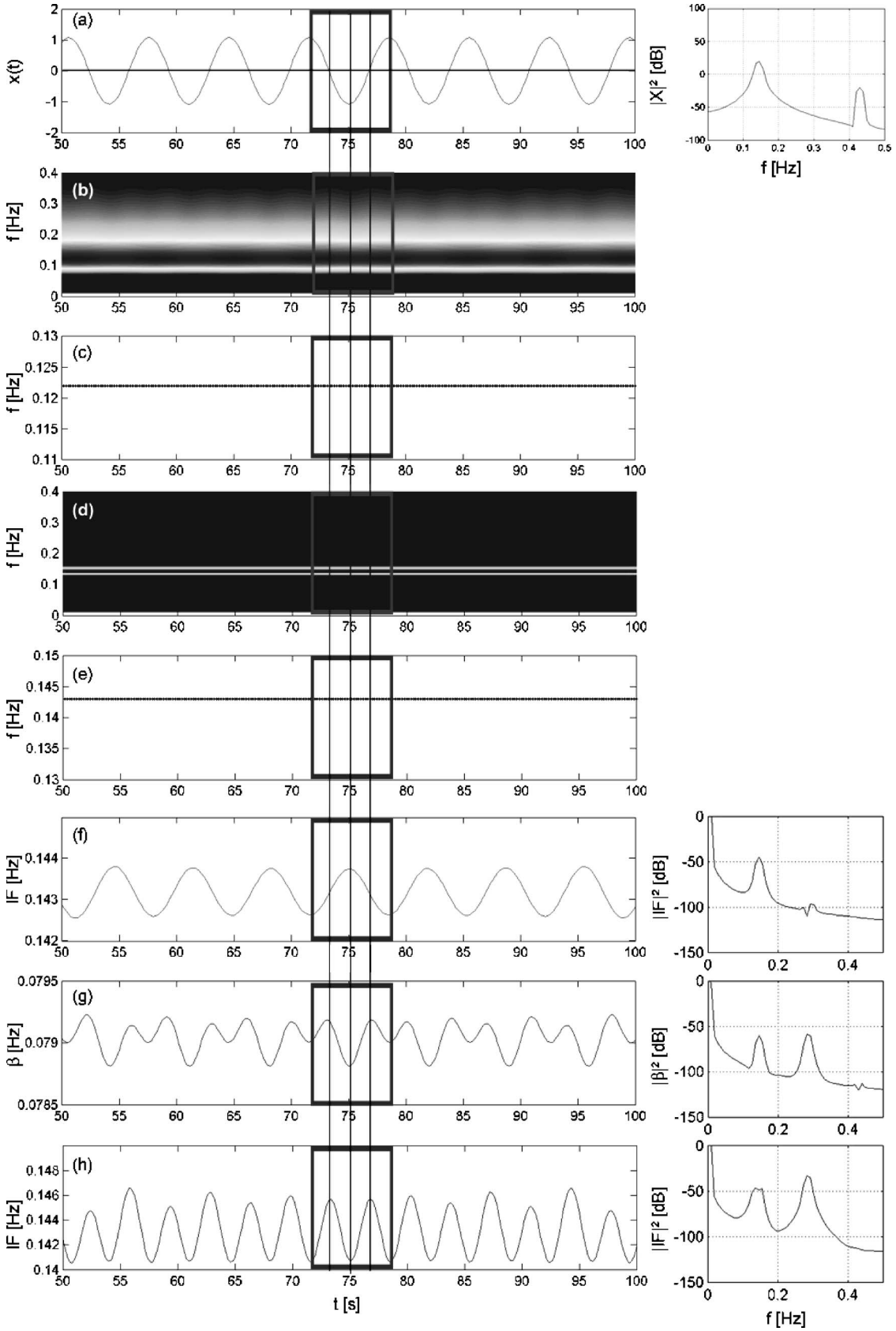

Fig. 1. (a) Duffing oscillator in free vibration, zoomed in from 50 to 100 s with power spectrum at right; (b) wavelet scalogram (f_0=0.25 Hz); (c) WIFS (f_0=0.25 Hz); (d) wavelet scalogram (f_0=2 Hz); (e) WIFS (f_0=2 Hz); (f) instantaneous frequency identified by wavelet phase with power spectrum at right (f_0=0.25 Hz); (g) wavelet instantaneous bandwidth with power spectrum at right (f_0=0.25 Hz); and (h) instantaneous frequency identified by Hilbert phase with power spectrum at right

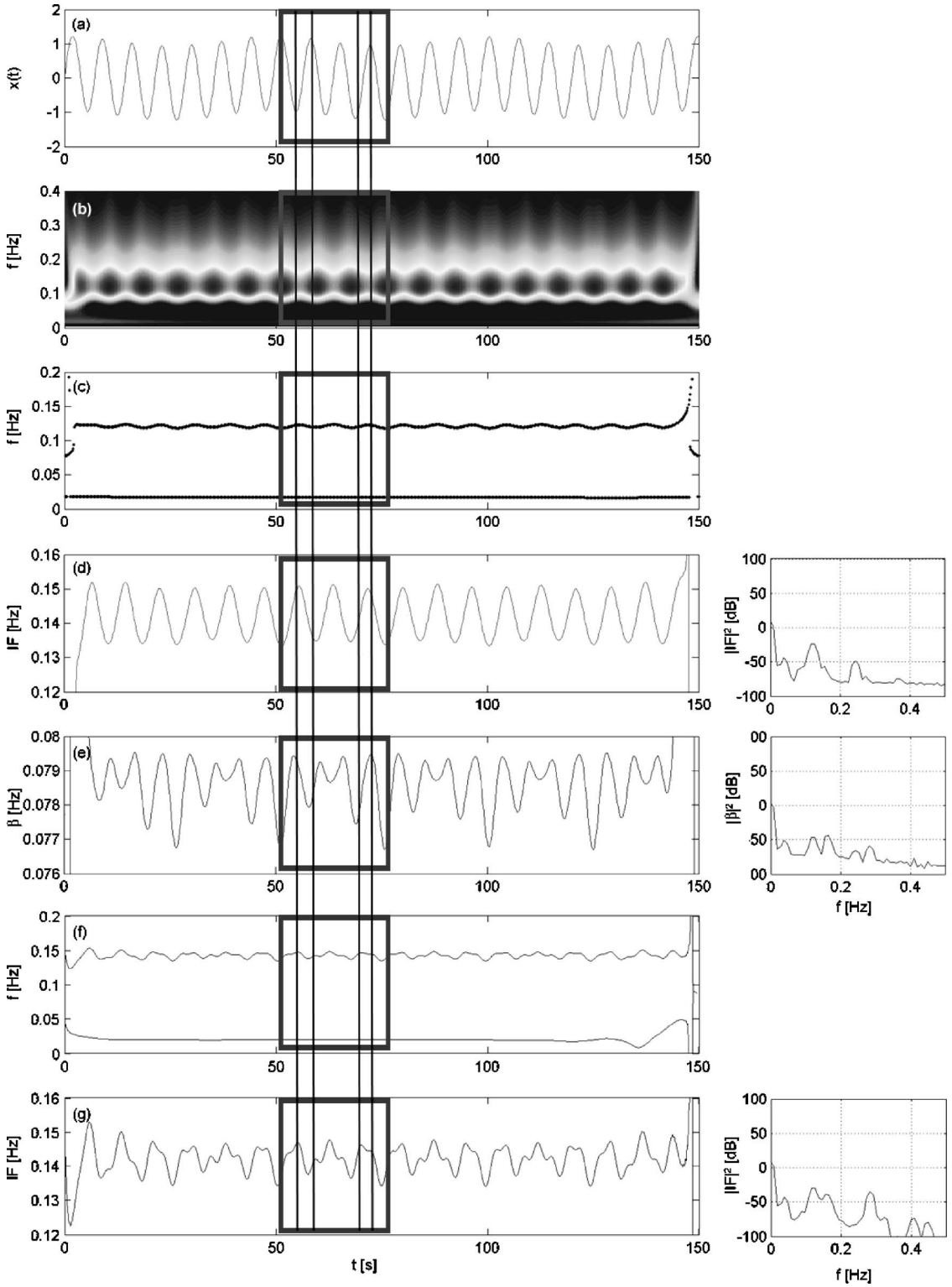

Fig. 2. (a) Duffing oscillator in forced vibration; (b) wavelet scalogram; (c) WIFS; (d) instantaneous frequency of high-frequency component identified by phase of WT with power spectrum at right; (e) wavelet instantaneous bandwidth of high-frequency component with power spectrum at right; (f) Hilbert spectrum; and (g) zoom in of Hilbert spectrum for first IMF with power spectrum at right

where the Duffing oscillator is essentially a linear system, while intermediate troughs occur at the signal maxima. These subtle bandwidth fluctuations are a result of the nonlinearity in frequency. A comparison of this result to the Hilbert transform's instantaneous frequency estimate, shown in Fig. 1(h), reveals that the oscillatory components detected here are the same as those detected by the wavelet instantaneous bandwidth, as the power spectral representation verifies oscillations at the instantaneous frequency (0.145 Hz) and near twice its value (0.284 Hz). Thus the periodicities in the nonlinear system are captured by both the wavelet bandwidth and the Hilbert instantaneous frequency. It is also noteworthy that the wavelet instantaneous

frequency did show a trace of the secondary nonlinear scale [see the PSD in Fig. 1(f)], but lacked the resolution to fully characterize it.

Looking at the forced response of the same system for $\omega_d = 1/50$ Hz in Fig. 2(a), the envelope of the signal now manifests a low frequency oscillation as a result of the forcing function. Inspection of the wavelet scalogram in Fig. 2(b) reveals that the signal is focused at 0.12 Hz with a second band at the heel of the scalogram representative of the 0.02 Hz forcing function. While the energy is clearly concentrated in the vicinity of the oscillator's dominant frequency, the higher frequencies of the scalogram manifest a rippling indicative of fluctuations in the frequency content with time. The instantaneous frequencies were identified from the ridges of the transform and are shown in Fig. 2(c). Two dominant components were observed: one near 0.12 Hz and one corresponding to the forcing frequency near 0.02 Hz. Turning again to the instantaneous frequency estimate from the wavelet's analytic signal phase in Fig. 2(d), the range of oscillation of the instantaneous frequency is identified more precisely about 0.142 Hz, consistent with the previous example. Note that the wavelet instantaneous frequency estimate manifests a smooth regular periodicity. Again recalling that the wavelet analysis fits small waves to the data, this instantaneous frequency estimate is more representative of the best-fit frequency over some short time interval but may not fully capture subcyclic characteristics, though the power spectral density to the right of Fig. 2(d) indicates oscillations of the instantaneous frequency at two scales. Focusing on the instantaneous bandwidth in Fig. 2(e), a different perspective with a far more oscillatory characteristic is evident due to the deviations from the mean frequency caused by subcyclic nonlinearity. The box in Fig. 2(a) denotes a region of downshift, during which the local signal mean shifts to lower amplitudes, followed by an upshift. Note that both the frequency and bandwidth qualitatively manifest local symmetry over the downshift region. The power spectral frequency content of the instantaneous bandwidth shows enhanced resolution over the wavelet instantaneous frequency, now discerning beating of modes at 0.12 and 0.16 Hz and at 0.24 and 0.28 Hz. This result can be compared to the instantaneous frequency estimated via EMD+HT. Two meaningful IMFs were identified, with the first being of higher energy and associated with the oscillator frequency while the second lower energy IMF was associated with the forcing frequency, as shown by the Hilbert spectrum in Fig. 2(f). Note the parallels with Fig. 2(c). The instantaneous frequency associated with the first IMF, shown in Fig. 2(g), depicts again an oscillatory pattern about 0.142 Hz, which does not separate the two contributors of frequency evolution like the wavelet result, and thus provides an instantaneous frequency estimate whose peaks and troughs shift and lean in a repeating pattern as a result of intrawave fluctuations. Its spectral representation denotes energy contributions in a beating pair of modes at 0.12 and 0.16 Hz, much like the wavelet bandwidth estimate, though noting more energy at 0.27 Hz. This example verifies that nonlinear energy content represented by the wavelet instantaneous bandwidth is consistent with the content in the Hilbert spectrum.

Lorenz System

The Lorenz equation, initially proposed to study deterministic nonperiodic flow, has been a widely studied system for the investigation of chaos. The system is described by

$$\dot{x} = -\sigma x + \sigma y \quad \dot{y} = rx - y - xz \quad \dot{z} = -bz + xy \tag{3}$$

where σ, r, and b=positive constants, assumed to be 10, 20, and 3, respectively, for the purpose of this example. The system is released from its initial position of (10, 0, 0), resulting in the x component response shown in Fig. 3(a), illustrating the transient characteristics of the system. The EMD+HT result generated by Huang et al. (1998) is provided in Fig. 3(f), which reveals the characteristic intrawave frequency modulation. Note the rapid decay of instantaneous frequency indicating supercyclic frequency modulation as well as the oscillations about 1.4 Hz due to subcyclic nonlinear behavior. Linearization of the system by Huang et al. (1998) yielded a dominant frequency of about 1.46 Hz—the mean frequency of the intrawave modulations.

The scalogram [Fig. 3(b)] indicates that it has captured the transient behavior, with the WIFS [Fig. 3(c)] providing an even more clear representation. Consistent with the EMD+HT result in Fig. 3(f), the Morlet wavelet with $f_0 = 0.5$ Hz, was capable of detecting the marked frequency shifts due to the transient behavior in the first few seconds of the signal. This is characterized by a shift in the low-frequency component from about 0.75 to 0.02 Hz. After this transition range, the wavelet detects a bimodal response, with the low-frequency response near 0.02 Hz and the oscillator's response at about 1.4 Hz, near the frequency of the linearized system. The estimation of instantaneous frequency of this mode becomes unreliable beyond 10–15 s, as the signal's energy decays, shown by the diminishing energy in the scalogram. This observation is consistent with the EMD+HT result in Fig. 3(f). The subcyclic oscillations about 1.4 Hz, occurring essentially in the decaying component of the response, are subtly evident in the WIFS in Fig. 3(c). To more closely inspect these subcyclic oscillations, the instantaneous frequency of this component is also identified from the wavelet analytic signal phase. The result, shown in Fig. 3(d), demonstrates that subtle oscillations are detected by the wavelet phase, though not of the magnitude detected by EMD+HT. The amplitude of wavelet coefficients of the higher frequency component in Fig. 3(b) fall beneath 10% of their maximum value by the 10th second, becoming essentially zero by the 20th second, again the result of the rapid decay in Fig. 3(a). The wavelet instantaneous bandwidth of the high-frequency Lorenz component is also presented in Fig. 3(e) and indicates an oscillatory pattern with the same periodicity as the instantaneous frequency, increasing from 0 to 6 s and then stabilizing. This is consistent with the EMD+HT result in Fig. 3(f), which also shows a definitive increase in the spread about the instantaneous frequency up to 6 s, followed by its stabilization.

Rössler System

The final nonlinear system investigated here is the Rössler system described by

$$\dot{x} = -(y + z) \quad \dot{y} = x + \tfrac{1}{5}y \quad \dot{z} = \tfrac{1}{5} + z(x + \mu) \tag{4}$$

where $\mu = 3.5$. The system simulated by a first-order forward difference technique from the initial conditions $(-4, 4, 0)$ is shown in Fig. 4(a). The EMD+HT analysis of this system by Huang et al. (1998) is provided in Figure 4(g). Note that the EMD of the data yielded two meaningful IMF components, the dominant one oscillating between 0.17 and 0.25 Hz.

Huang et al. (1998) states that in order "to represent such a [system] with either Fourier spectrum or wavelet analysis, one

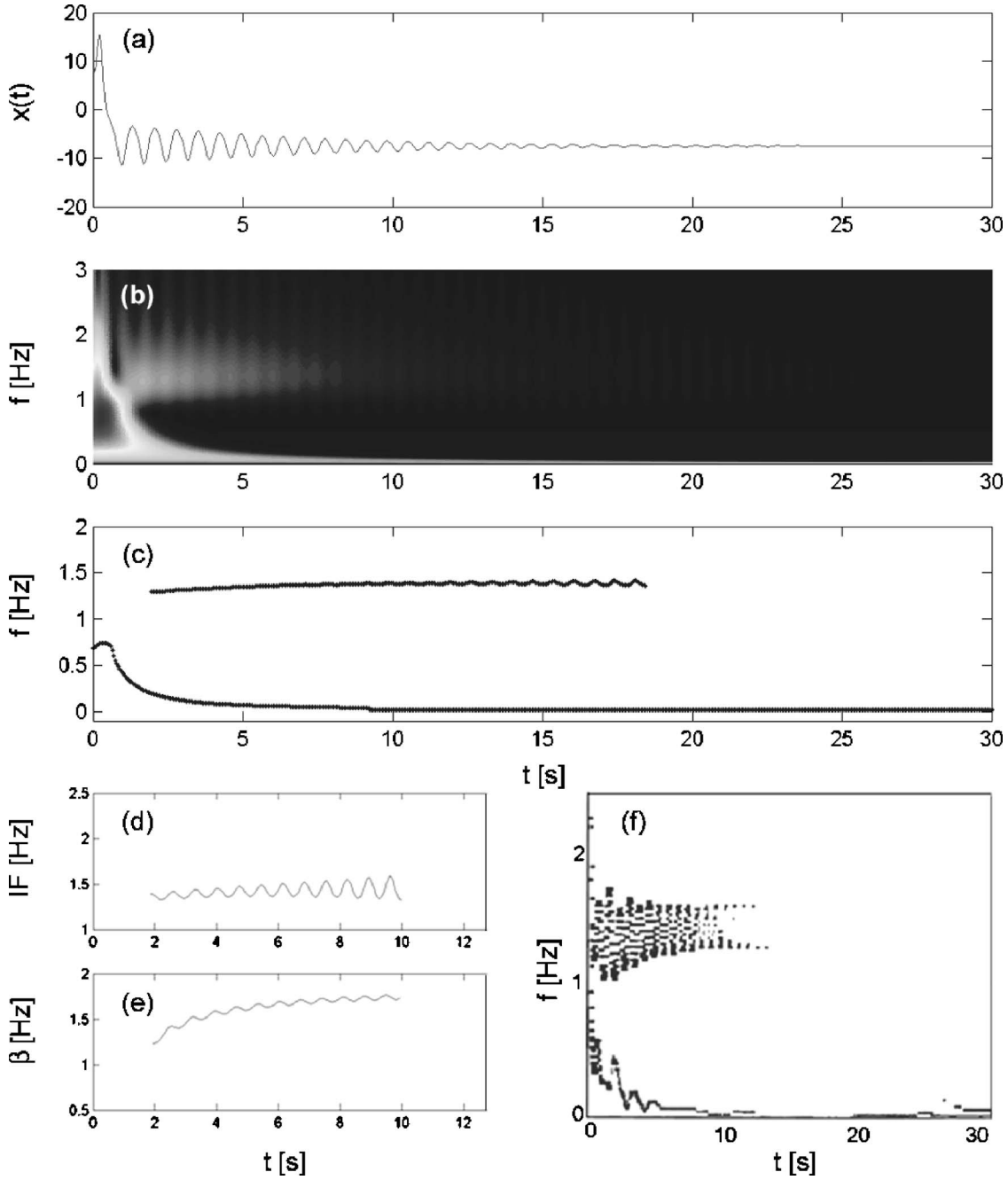

Fig. 3. (a) Lorenz system x component; (b) wavelet scalogram; (c) WIFS; (d) instantaneous frequency of high-frequency component (via wavelet phase); (e) instantaneous bandwidth of high-frequency component; and (f) EMD+HT result (adapted from Huang et al. 1998)

would need many harmonics." Indeed, a continuous wavelet analysis may globally represent this system by a series of harmonics if the temporal resolutions are insufficient to resolve the nonlinearities, i.e., by selecting a large f_0. The necessary resolution to avoid this can be determined by conducting a wavelet analysis in tiers, using a fine frequency resolution in Stage 1 to first identify the dominant components. This can be achievedusing $f_0=5$ Hz which yields two distinct components around 0.09 and 0.17 Hz, demonstrated in Figs. 4(b and c). This information then defines two frequency ranges over which to apply a more temporally refined analysis in Stage 2. The first component, due to its low energy, near 0.1 Hz was cited by Huang et al. (1998) as some numerical artifact from the simulation of the system. As this component does not manifest marked temporal variation in the refined analysis, it will not be included in subsequent discussions. To track the time-evolving amplitude changes of the component near 0.17 Hz a $f_0=0.25$ Hz wavelet analysis is conducted in Stage 2, resulting in the scalogram in Fig. 4(d). Note that the contours of the wavelet scalogram mimic the same oscillatory peaking of the frequency observed in the EMD+HT result in Fig. 4(g). The Stage 2 WIFS is generated in Fig. 4(e) and reveals that the energy is primarily concentrated in an oscillatory pattern between 0.137 and 0.166 Hz, with a period of oscillation of 11.4 s.

As the scalogram fluctuations in the high-frequency range indicate some variation of energy in time, an instantaneous bandwidth analysis is performed. The results, shown in Fig. 4(f), clearly demonstrate the behavior identified in Fig. 4(g), with large

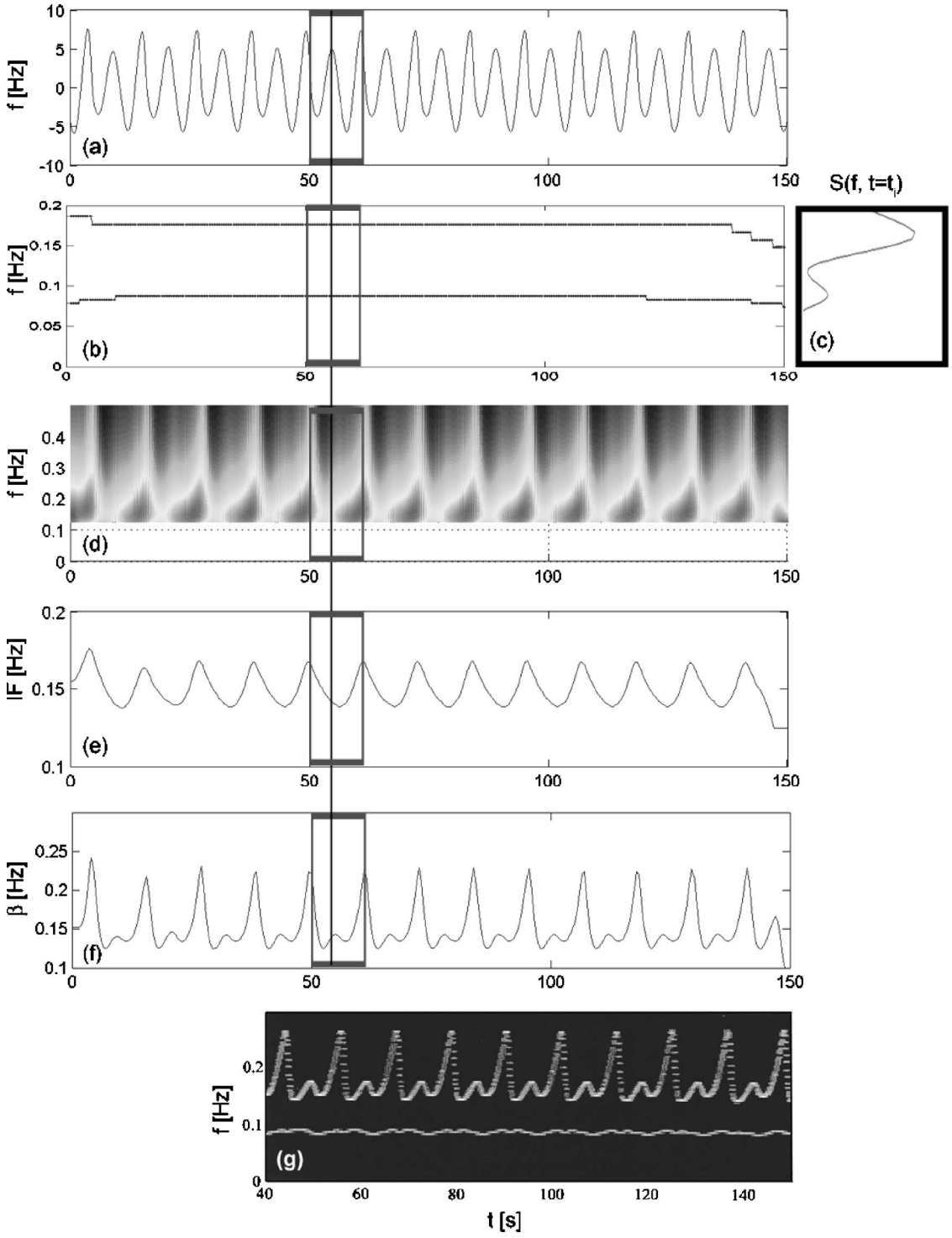

Fig. 4. (a) Rössler system x component; (b) WIFS for analysis Stage 1; (c) sample instantaneous spectra; (d) wavelet scalogram for analysis Stage 2; (e) WIFS for analysis Stage 2; (f) instantaneous bandwidth for analysis Stage 2; and (g) EMD+HT result (adapted from Huang et al. 1998)

peaks interlaced with smaller, rounded humps. Thus the dual identification of instantaneous frequency and bandwidth from the wavelet transform illustrates the ability of the Morlet wavelet to characterize this nonlinear behavior, albeit differently than EMD+HT, and questions the claim in Huang et al. (1998) that "no other methods can match the resolution power displayed here."

Conclusions

This study examined the characterization of nonlinearities by the continuous wavelet transform and empirical mode decomposition with Hilbert transform. During the course of these discussions, an important distinction between these two techniques was noted: the Morlet wavelet's instantaneous frequency is only capable of

detecting nonlinearities in its truest mean sense, as it locally fits windowed sinusoids to the data and is thus capable of detecting only nonlinearities evolving over entire cycles of oscillation or following significant changes in amplitude, referred to as supercyclic oscillations. Deviations from this mean frequency, carried in the wavelet instantaneous bandwidth, are then capable of capturing subcyclic oscillations. In contrast, EMD+HT carries both super and subcyclic oscillations within its instantaneous frequency estimate. It is shown in the example of the Duffing oscillator that the spectral content of the wavelet instantaneous bandwidth measure is consistent with that of the Hilbert instantaneous frequency. Further, the nonlinear characteristics carried in the wavelet instantaneous bandwidth and the Hilbert transform instantaneous frequency are shown to have the identical oscillatory signature in the case of the Rössler system.

Acknowledgments

The writers gratefully acknowledge support in part from NSF Grant No. CMS 03-24331, the NASA Indiana Space Grant, and the Center for Applied Mathematics at the University of Notre Dame. The assistance of Ms. Lijuan Wang of the University of Notre Dame in processing the forced Duffing oscillator example is also acknowledged.

References

Bendat, J. S., and Piersol, A. G. (1986). *Random data analysis and measurement procedures*, 2nd Ed., Wiley, New York.

Carmona, R., Hwang, W.-L., and Torresani, B. (1998). *Practical time-frequency analysis*, 1st Ed., Academic, New York.

Cohen, L., and Lee, C. (1990). "Instantaneous bandwidth for signals and spectrogram." *Intl. Conf. on Acoustics, Speech and Signal Processing*, ICASSP-90, 5, 2451–2454, April 3–6, 1990, Albuquerque, N.M.

Huang, N. E., et al. (1998). "The empirical mode decomposition and the Hilbert spectrum for nonlinear and nonstationary time series analysis." *Proc. R. Soc. London*, 454, 903–995.

Hwang, P. A., Huang, N. E., and Wang, D. W. (2003). "A note on analyzing nonlinear and nonstationary ocean wave data." *Appl. Ocean. Res.*, 125(4), 187–194.

Kijewski, T., and Kareem, A. (2003). "Wavelet transforms for system identification in civil engineering." *Comput. Aided Civ. Infrastruct. Eng.*, 18, 341–357.

Kijewski-Correa, T. (2003). "Full-scale measurements and system identification: A time-frequency perspective." Ph.D. thesis, Univ. of Notre Dame, Notre Dame, Ind.

Kijewski-Correa, T., and Kareem, A. (2006). "Efficacy of Hilbert and wavelet transforms for time-frequency analysis." *J. Eng. Mech.*, 132(10), 1037–1049.

Peng, Z. K., Tse, P. W., and Chu, F. L. (2005). "A comparison study of improved Hilbert-Huang transform and wavelet transform: Application to fault diagnosis for rolling bearing." *Mech. Syst. Signal Process.*, 19, 974–988.

Priestley, M. B. (1988). *Nonlinear and nonstationary time series analysis*, 1st Ed., Academic, San Diego.